THE ASTROPHYSICAL JOURNAL, 239:815–838, 1980 August 1

COLOR-MAGNITUDE PHOTOMETRY TO THE MAIN SEQUENCE FOR THE "ANOMALOUS" GLOBULAR CLUSTER PALOMAR 12[1]

WILLIAM E. HARRIS[2]
Department of Physics, McMaster University

AND

R. CANTERNA[2]
Department of Astronomy, University of Washington; and Department of Physics and Astronomy, Louisiana State University
Received 1979 October 19; accepted 1980 February 12

ABSTRACT

New photoelectric and photographic color-magnitude photometry to $V = 22$ is presented for the globular cluster Palomar 12. The C-M diagram morphology most closely resembles 47 Tucanae, and all combined evidence suggests that Pal 12 is a moderately metal-rich cluster in agreement with the recent red-giant abundance studies by Cohen. We derive a preliminary age estimate of 11×10^9 years for Pal 12 by fitting our main-sequence data to the Yale isochrones in the $(M_V, B - V)$-plane. At 14 kpc from the galactic center ($V_{HB} = 17.1$, $E_{B-V} = 0.02$), Pal 12 is now easily the most remote of the known "metal-rich" or G-type globular clusters. From new estimates of the cluster structural parameters (tidal radius, central concentration, total mass), we note that Pal 12 now appears to be near its perigalactic distance and thus may spend most of its time even further out in the halo.

The stellar luminosity function $\phi(M_V)$ and its radial dependence within Pal 12 are discussed briefly. Although the overall ϕ-curve is roughly similar to those of other globular clusters (for $M_V < +5$), evidence of radial population segregation exists: the giant-branch stars are noticeably more centrally concentrated than the main-sequence and turnoff stars, suggestive of dynamical relaxation effects.

Subject heading: clusters: globular

I. INTRODUCTION

Much recent interest in the observational study of globular clusters has centered on the "anomalous" Population II systems found in the outermost parts of the halo. These objects, which include primarily the Palomar clusters and the dwarf spheroidal systems, display a combination of uniquely peculiar characteristics (for summaries, see Harris 1976; Zinn 1978; Stetson 1979) which set them strongly apart from the great majority of "normal" globular clusters within $R \approx 20$ kpc of the galactic center. Even with the earliest color-magnitude studies of the outermost halo systems (Burbidge and Sandage 1958; Baade and Swope 1961; Sandage and Wildey 1967), it was clear that many of them shared combinations of very low metallicity, red horizontal branches, and moderately red yet steep giant branches, which were not found elsewhere in the Galaxy.

Suggestions advanced to explain the combined properties of such clusters at first included abnormal helium abundances or ratios of CNO and Fe (e.g., Sandage and Wildey 1967; Hartwick and McClure 1972), perhaps resulting from the chance that the most distant part of the halo did not participate in the same detailed chemical enrichment process as did the inner halo region during the initial protogalactic collapse phase. Another frequent and increasingly popular hypothesis has been that a given anomalous system might have much lower age or a significant spread of ages among its stars (Rood and Iben 1968; Castellani 1975; Demarque and Hirshfeld 1975; Norris and Zinn 1975; Harris 1976; Searle and Zinn 1978). There is in addition the possibility that several of them may belong to a separate dynamical subsystem of the halo (Kunkel and Demers 1976*b*; Lynden-Bell 1976; Hartwick and Sargent 1978; Kunkel 1979) and thus may not even have been formed in the same collapse phase that is conventionally described as giving birth to the normal globular cluster system. These options, and others, have remained speculative because of the primitive state of the observational data currently available for these distant and difficult-to-study objects.

It is particularly critical that no photometry reaching the main-sequence turnoff region has yet been available for any of the anomalous clusters. Without

[1] *Contributions of the Louisiana State University Observatory No.* 156.

[2] Visiting Astronomer, Cerro Tololo Inter-American Observatory, supported by the National Science Foundation under contract AST 74-04128.

such data it is extremely difficult to disentangle the effects of differing age, helium abundance, and metallicity, all of which affect the morphology of the brighter sections of the color-magnitude diagram (horizontal branch and giant branch) in complex fashion. We therefore began the work reported here with the aim of obtaining well-calibrated deep photometry for one of the anomalous systems, and with the hope that the results could be used to narrow down the choice of underlying physical parameters for the cluster.

The object we selected for study was Palomar 12 ($\alpha = 21^h43^m.7$, $\delta = -21°28'$ [1950]; $l = 31°$, $b = -48°$), a cluster with no previously published color-magnitude diagram (CMD). It is a sparse object structurally similar to several to several other previously known "anomalous" systems (e.g., Pal 3, 4, 13), and previous rough estimates (see Harris 1976) placed it ~ 50 kpc from the galactic center, distant enough to be a good candidate for an "anomalous" system but still close enough to the Sun that an attempt at main-sequence photometry would not be hopeless. Furthermore, Pal 12 is located in a high-latitude field and so any physical conclusions from the data would not be affected by large reddening corrections or field-star contamination.

In late 1975 at Cerro Tololo we obtained data which proved sufficient to establish the CMD of Pal 12 to the required faint absolute-magnitude level. In the following sections, we describe the photoelectric and photographic photometry which we obtained (§ II); the resulting CMD (§ III); the cluster distance, reddening, and integrated properties (§ IV–VI); and finally an analysis of its abundance characteristics and age determination (§ VII). Rather than yielding clear answers to our originally intended questions about cluster ages in the outer halo, we shall find below that our analysis of Pal 12 has led us into connection with a number of other problems related to recent trends in globular cluster abundance studies.

II. OBSERVATIONAL DATA AND REDUCTIONS

a) Photoelectric Photometry

During 1975 August and October, we obtained *UBV* photoelectric photometry down to $V \approx 18$, $B \approx 19$ for 42 stars in the Pal 12 field with the CTIO 1.5 m telescope. All the measurements were carried out with a 1P21 phototube and conventional filters, and were transformed to the Johnson *UBV* system by standard and extinction stars taken from the lists of Cousins (1973) and Crawford, Golson, and Landolt (1971). Typically ~ 20 different standards were observed each night, and both the extinction and transformation coefficients were determined each night. The internal random errors of the standard stars (for one night) were $\sigma_v = 0.015$, $\sigma_{B-V} = 0.015$, $\sigma_{U-B} = 0.030$.

The sequence stars established in the Pal 12 field are identified in the finder charts of Figures 1 and 2. Their photoelectric colors and magnitudes are given in Table 1, along with the number of nights n that each was measured. In Table 2 we summarize the expected internal errors for the photoelectric measurements as a function of V magnitude range; the listed σ's are the standard errors for a *single* measurement as estimated from the night-to-night variations and should therefore be divided by $n^{1/2}$ when applied to individual stars in Table 1. Since the Pal 12 field is at relatively high latitude, contamination of the photon counts by faint background stars ($V \gtrsim 20$) proved to be virtually absent, so that the internal photometric errors for the sequence stars are due principally to photon statistics.

b) Photographic Photometry

During the same observing runs at Cerro Tololo we obtained a series of photographic plates in *B* and *V*

TABLE 1

PHOTOELECTRIC SEQUENCE STARS

Star	V	$B-V$	$U-B$	n
1	14.58	1.58	+1.80	4
2	14.83	1.51	+1.58:	2
3	17.87:	0.34:	...	1
4	17.84	0.82	+0.29:	2
5	17.82	0.75	+0.21:	2
6	12.36	0.58	+0.01	5
7	11.68	0.86	+0.57	5
8	14.22	0.85	+0.44	5
9	11.21	0.77	+0.37	7
10	11.03	0.32	+0.09	5
11	10.87	0.82	+0.38	2
12	16.59	0.77:	+0.02	2
13	12.99	0.77	+0.45	4
14	16.89	0.84	+0.16	1
15	13.68	1.66	+1.20	4
16	12.59	0.58	−0.03	3
17	14.67	0.62	+0.04	2
18	16.00	0.78	+0.09:	2
19	11.22	0.59	+0.05	3
20	11.63	1.17	+1.18	3
21	10.52	1.14	+1.07	3
22	9.60	1.46	+1.29	2
23	15.61	1.58	+1.28:	1
24	14.62	0.80	+0.17:	2
25	12.26	0.65	+0.04	3
26	14.30	0.65	+0.05	2
27	12.28	0.76	+0.28	3
28	13.98:	1.35	+1.35	2
29	14.18	0.55	−0.07	2
30	13.41	0.90	+0.54	3
31	15.27	0.78	+0.35	2
32	11.92	1.08	+0.99	3
33	17.05	0.60	+0.08	1
34	11.25	0.48	+0.01	2
35	11.44	1.06	+0.96	2
36	12.97	0.60	+0.08	2
37	14.88	0.61	+0.00	2
38	13.00	0.58	+0.00	2
39	12.36	1.26	+1.14	2
40	13.63	0.71	+0.20	2
41	13.05	0.61	+0.06	2
42	15.76	0.63	+0.03	2

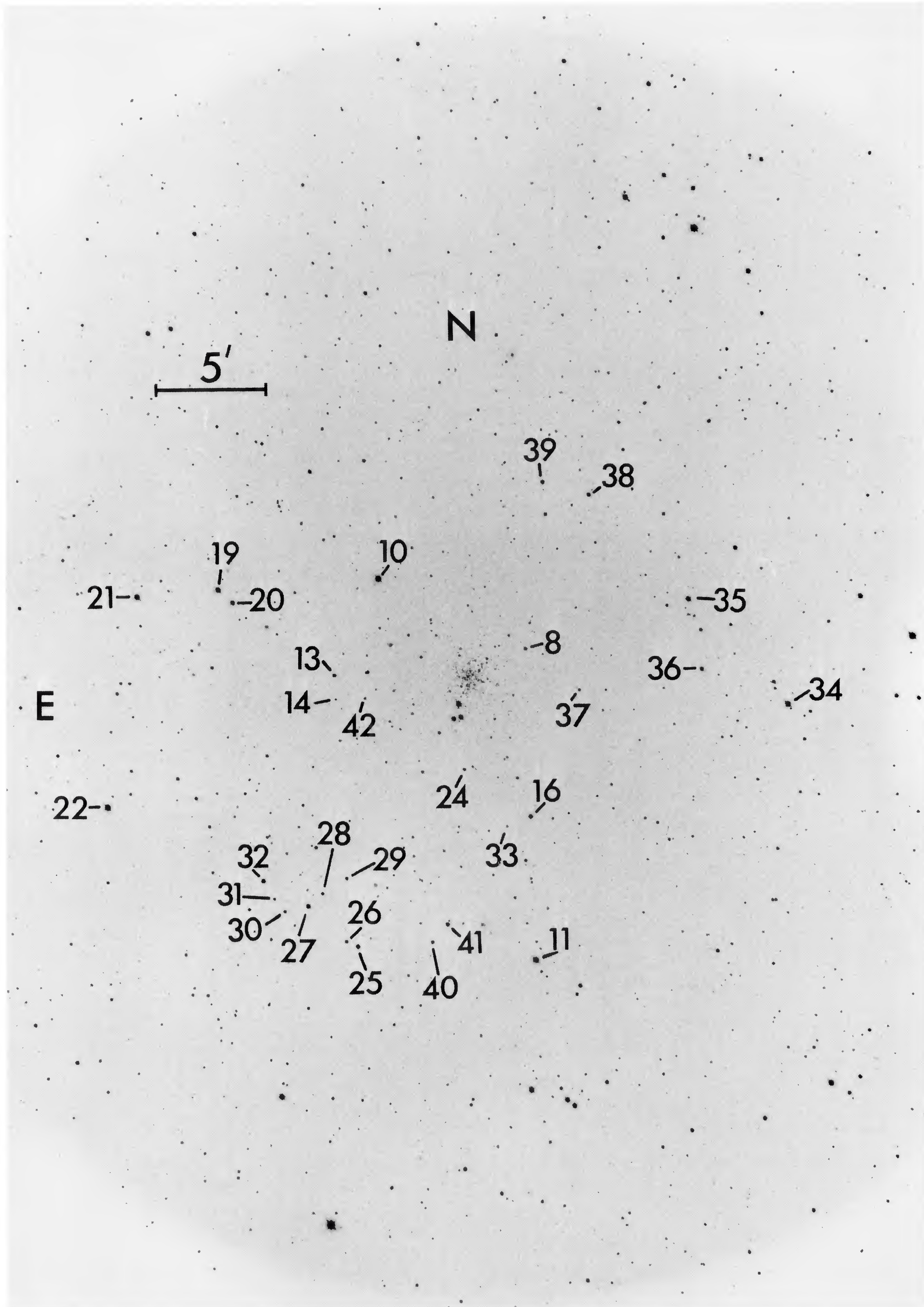

FIG. 1.—Wide-field photoelectric standards for Palomar 12. The star numbers are as listed in Table 1. This photographic reproduction, and the others in Figures 2–4 are from plate no. 1212 (103aD + GG385) taken with the CTIO 4 m telescope.

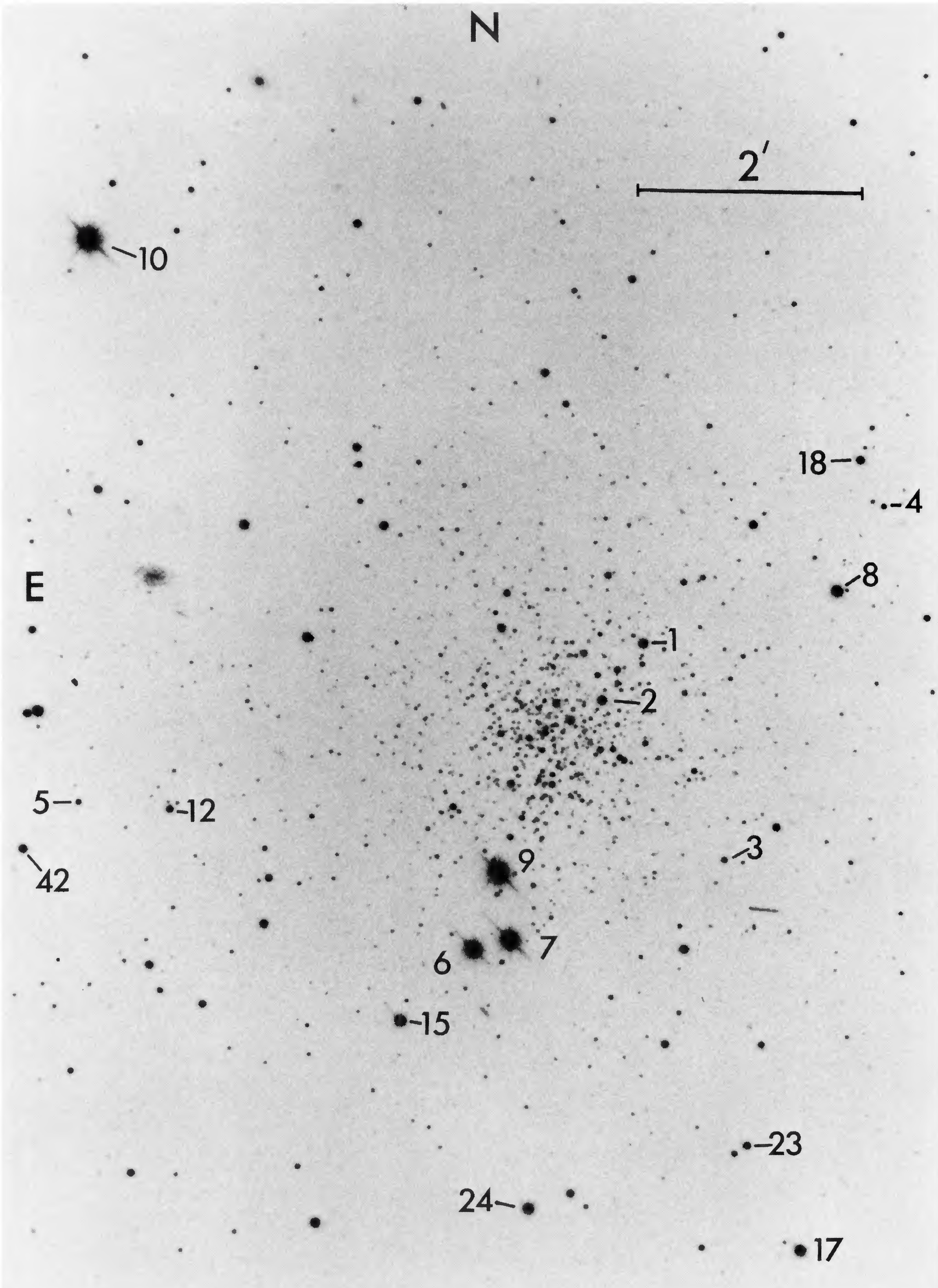

FIG. 2.—Inner photoelectric standards for Palomar 12

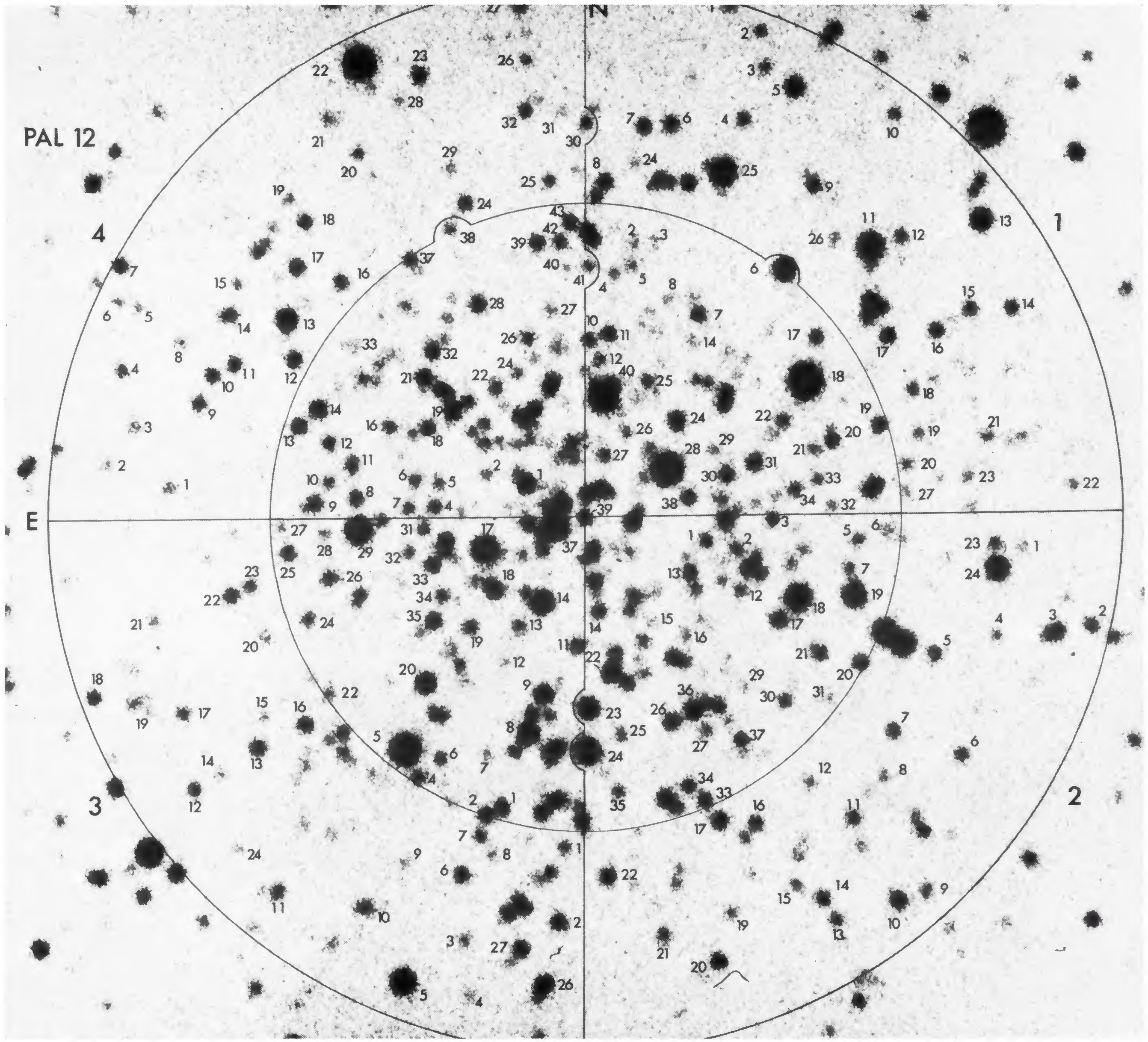

FIG. 3.—Identification chart for the photographically measured stars in rings 1 and 2. Ring 1 is innermost. Quadrant numbers 1–4 are marked outside the edge of ring 2.

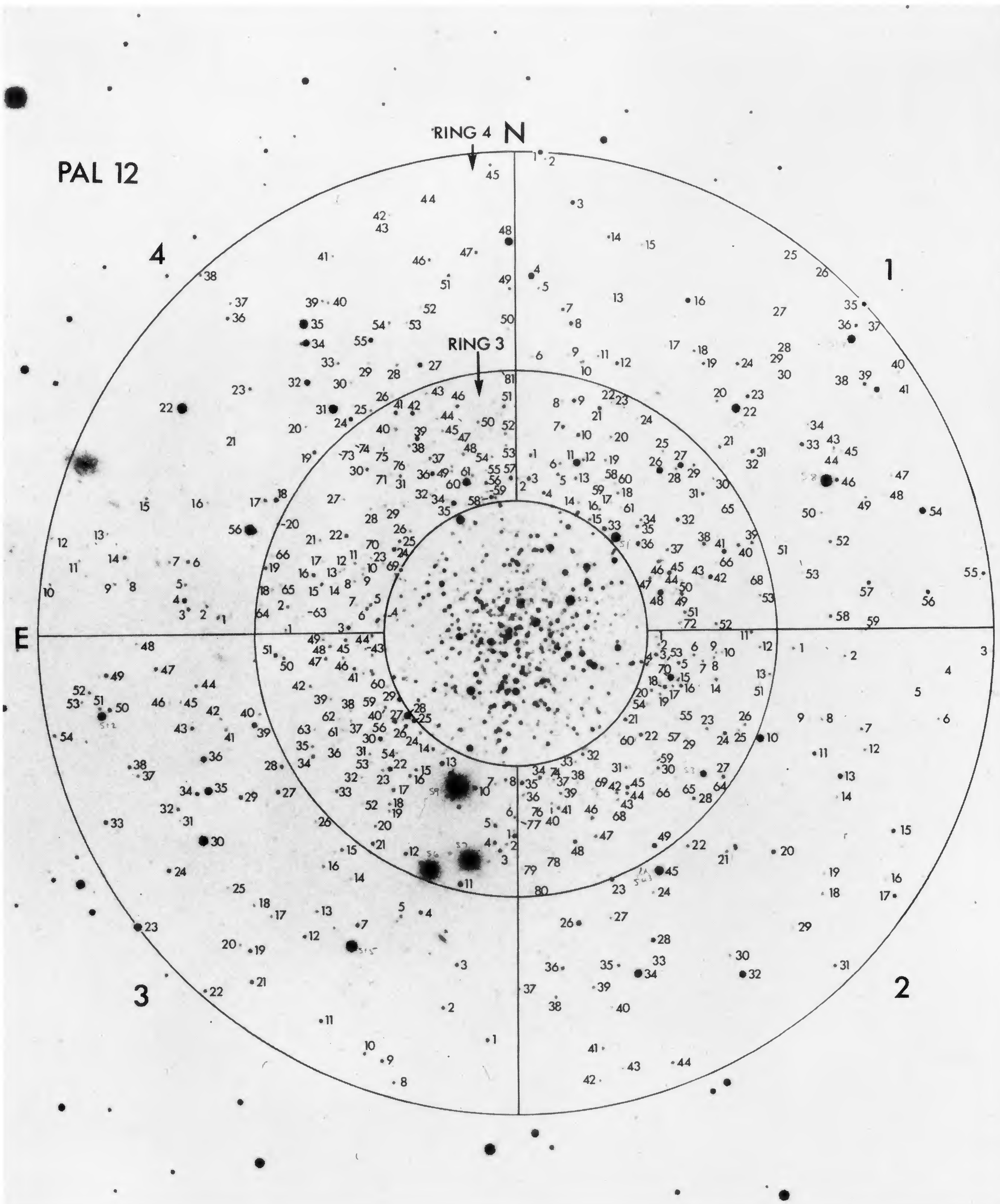

FIG. 4.—Identification chart for stars in rings 3 and 4. The radii of the four rings, in minutes of arc, are $R_1 = 0\overset{'}{.}7$, $R_2 = 1\overset{'}{.}1$, $R_3 = 2\overset{'}{.}2$, $R_4 = 4\overset{'}{.}0$.

TABLE 2

INTERNAL ERRORS OF THE PHOTOMETRY

V Range	σ_V	σ_{B-V}	σ_{U-B}
Photoelectric Photometry			
<13	0.020	0.017	0.030
13–15	0.030	0.017	0.036
>15	0.08:	0.10:	0.08:
Photographic Photometry			
<18	0.02	0.03	...
18–19	0.03	0.04	...
19–20	0.04	0.05	...
>20	0.05	0.06	...

with the 4 m and 1.5 m telescopes which proved deep enough to carry out the intended color-magnitude study. A summary of the plate material used is listed in Table 3. With the exception of one BV 4 m plate pair, all exposures were made with the auxiliary 6 inch CTIO "Racine prism" mounted on the telescope. This prism was used to produce faint secondary images of all the brighter stars in the field (Racine 1969).

Since Pal 12 has such low stellar density, it was possible to carry out iris photometry of the photographic plates all the way in to the cluster center. We marked the cluster area into four concentric rings and labeled all uncrowded stars, down to the limit of the deepest plates, for subsequent measurement; the selected program stars are identified on the charts of Figures 3 and 4. We measured the plates with the Cuffey iris photometer at the University of Waterloo and completed the reductions with a computer program using the procedure described by Stetson and Harris (1977).[3]

The secondary images produced by the Racine prism proved to be of excellent photometric quality and were used to fix the magnitude scale of the photographic calibration curves for $V > 18$ and $B > 19$, down to the plate limits. The magnitude difference Δm between the primary and secondary images of the photoelectric standards was determined by drawing up calibration curves separately for each individual plate and then adopting the average Δm for the final reduction of the entire set of plates. For the 4 m plates we found $\overline{\Delta m} = 6.80 \pm 0.05$, and for the 1.5 m plates $\overline{\Delta m} = 4.70 \pm 0.05$, which agree with the expected values from the relative sizes of the prism and primary mirror in each telescope. We found no differences in Δm larger than 0.1 mag from plate to plate, or between any two plates of different colors. Because the secondary-image calibration is critically important to our present study,

[3] A substantially revised and thoroughly documented version of this reduction program is now available on request from W. E. H. It is suitable for 2- or 3-color photographic photometry on quite a general basis.

TABLE 3

PHOTOGRAPHIC PLATE MATERIAL

Plate Number	Telescope (m)	Emulsion	Filter	Exposure (min)
1211[a]	4	103aD	GG495	15
1212[a]	4	103aO	GG385	15
2255	4	IIaO	GG385	20
2279	4	IIaO	GG385	30
2298	4	IIaO	GG385	45
2328	4	IIaO	GG385	30
2329	4	IIaO	GG385	15
2340	4	IIaO	GG385	30
2256	4	IIaD	GG495	20
2278	4	IIaD	GG495	30
2330	4	IIaD	GG495	30
2331	4	IIaD	GG495	15
2341	4	IIaD	GG495	30
2692	1.5	103aD	GG14	120
2698	1.5	103aD	GG14	60
2693	1.5	103aO	GG385	60

[a] Without Racine prism.

we present sample calibration curves (iris reading versus photographic magnitude) in Figure 5 as an example of their use. Here, the plotted iris reading is the *mean* value for each standard star averaged over all plates in the given color (cf. Stetson and Harris 1977), and the plotted magnitudes are in the natural photographic system of the plates (see below).

Figure 5 demonstrates that the relation between magnitude and iris reading has been *internally* well defined over the entire range of interest, and that the adopted $\overline{\Delta m}$ value is satisfactorily determined even though only a 1 mag overlap between the primary and secondary images is available. (For the 1.5 m plates, of course, more than 3 mag of overlap are available since Δm is correspondingly smaller.) We may also note from Figure 5 that it is evidently possible, with quite conventional plate material and measuring techniques, to carry out precise photographic photometry over an intensity range of at least 12 magnitudes.

It is clear that the *systematic* accuracy of the photographic photometry for $V \gtrsim 19$ also depends heavily on the secondary-image technique, i.e., on the photometric quality of the images and the validity of assuming a Δm value which is constant with magnitude. However, no systematic *color* errors in the final data larger than $\Delta(B - V) \approx 0.05$ due to the secondary-image calibration above should be present: this is because the Racine prism is achromatic, so that any minor residuals with color in a graph of $[(B - V)_{pg} - (B - V)_{pe}]$ versus V for the standard stars (including all the faint secondary images) can be removed by requiring the color of each secondary image to be the same as its primary. As for the $\overline{\Delta m}$ value itself, virtually identical results of $\Delta m = 6.8$ to 6.9 have been obtained for the CTIO prism and 4 m telescope by other authors, with the expected minor variations due to different parts of the primary mirror surface being

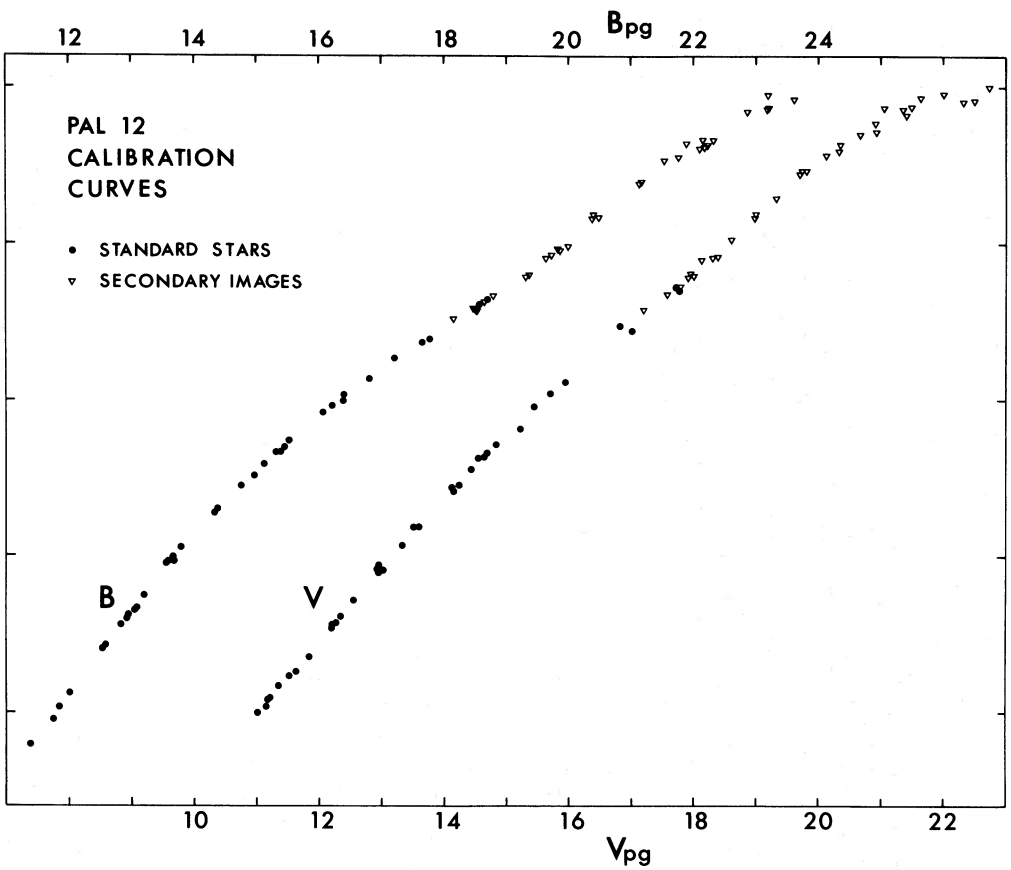

FIG. 5.—Calibration curves for the iris photometry of the photographic plates, showing the use of the secondary images created by the Racine prism. The photographic magnitude (B_{pg} or V_{pg}) of each standard star is plotted against its mean iris reading averaged over all plates in the color concerned. Standard stars are plotted as dots and their secondary images as triangles. The vertical scale representing the iris reading is arbitrary, but directed so that faint stars are at top.

sampled by the prism in different runs (Hodge 1977, private communication; Carney 1980; Christian and Janes 1979; Kunkel and Demers 1976*a*). The excellent plate-to-plate agreement for Δm, as well as the internal consistency of certain features in the resulting CMD (see § III below), also give confidence that no magnitude errors larger than $\Delta V \approx 0.1$ mag are present. Nevertheless, there is no doubt that additional direct photoelectric faint calibration would be highly desirable.

The standard stars also spread over a wide enough range of colors that reliable values of the transformations from photographic to photoelectric magnitudes (color equations) could be measured. If we write the photographic magnitudes as $m_{pg} = m_{pe} + k(B - V)$, then the transformation constants k for our plate material were found to be $k_V = -0.09$, $k_B = 0.02$ (4 m plates) and $k_V = -0.10$, $k_B = 0.10$ (1.5 m plates) with estimated errors of ± 0.02 for each.

The final (V, $B - V$) values for all 700 program stars are listed in Table 4, and the expected internal errors of the photographic photometry are summarized again in Table 2. In Table 4, the first digit of each star identification number is its ring number (ring 1 innermost), the second digit specifies its quadrant (1 through 4 in each ring as labeled on the finder charts), and the last two digits give the star number within the ring and quadrant.

III. THE COLOR-MAGNITUDE DIAGRAM

The CMDs in rings 1–4, from the 4 m plate material only, are displayed separately in Figures 6*a*–*d*. Because of the sparseness of the cluster, no one ring gives a complete or well defined impression of all the principal CMD sequences (giant and horizontal branches, subgiants, turnoff, and main sequence), but the main-sequence turnoff does appear clearly at V $\approx$ 20, $B - V \approx 0.6$ in all four diagrams. The low foreground field star density means that the vast majority of all stars *except* in ring 4 (the largest and outermost ring) are cluster members.

Although there do not seem to be any noticeable systematic trends in magnitude or color between different rings (since the mean locations of all the CMD features are virtually identical in all rings), the data in ring 1 have slightly higher random errors and hence more scatter compared with the other diagrams. Ring 1 also has a brighter effective limit ($V \sim 21$ as opposed

TABLE 4

PHOTOGRAPHIC PHOTOMETRY FOR 700 STARS IN PAL 12

STAR	V	B−V	STAR	V	B−V	STAR	V	B−V	STAR	V	B−V
1102	21.46	.35	1237	19.96	.59	1443	20.01	.44	2310	20.19	.49
1103	22.00	.15	1301	19.75	.47	2101	21.01	.53	2311	20.37	.51
1104	20.98	.60	1302	19.60	.66	2102	21.06	.56	2312	20.47	.52
1105	20.98	.57	1304	20.16	.37	2103	20.92	.59	2313	19.75	.55
1106	17.64	1.05	1305	15.86	1.10	2104	20.46	.68	2314	21.54	.62
1107	19.91	.52	1306	20.30	.65	2105	18.65	.82	2315	21.22	.96
1108	21.36	.71	1307	21.10	.81	2106	19.64	.73	2316	20.05	.41
1110	20.01	.57	1308	17.92	.79	2107	19.94	.52	2317	20.65	.62
1111	19.84	.58	1309	18.63	.70	2108	19.94	.63	2318	20.15	.57
1112	20.50	.60	1311	19.77	.55	2109	20.02	.60	2319	20.89	.28
1114	21.23	.90	1312	21.66	.71	2110	20.73	.67	2320	21.14	.68
1117	20.08	.57	1313	20.40	.60	2111	17.04	.76	2321	21.40	.53
1118	14.79	1.52	1314	17.69	.84	2112	20.43	.83	2322	20.09	.62
1119	19.91	.49	1317	16.87	.92	2113	18.03	.86	2323	20.58	.42
1120	19.85	.44	1318	18.94	.41	2114	20.32	.52	2324	21.66	.62
1121	20.76	.46	1319	20.10	.52	2115	20.33	.43	2326	19.47	.24
1122	20.24	.54	1320	18.28	.87	2116	20.10	.54	2327	19.72	.69
1124	19.33	.55	1322	20.93	.54	2117	19.53	.80	2401	20.95	.74
1125	20.25	.51	1324	20.51	.53	2118	20.59	.62	2402	21.52	.57
1126	20.61	.60	1325	20.08	.48	2119	20.90	.65	2403	21.03	.81
1127	20.30	.36	1326	20.15	.46	2120	20.83	.64	2404	20.64	.62
1128	15.35	1.26	1327	21.18	.81	2121	20.89	.62	2405	21.31	.83
1129	20.92	.63	1328	21.04	.58	2122	21.16	.56	2406	21.40	.58
1130	19.66	.50	1329	17.06	.79	2123	21.07	.78	2407	20.28	.48
1131	19.27	.79	1331	20.50	.52	2124	21.41	.86	2408	21.08	.76
1132	21.32	.42	1332	20.63	.65	2125	17.12	.73	2409	20.59	.45
1133	20.60	.68	1333	19.75	.41	2126	20.61	1.05	2410	20.29	.50
1134	20.17	.66	1334	20.25	.64	2127	19.89	1.19	2411	20.26	.56
1138	19.60	.54	1335	19.72	.38	2201	21.34	.68	2412	19.90	.57
1139	19.66	.53	1337	16.50	.95	2202	20.27	.53	2413	18.13	.84
1140	16.15	.90	1401	18.93	.47	2203	18.30	1.49	2414	20.28	.56
1201	20.26	.42	1402	20.66	.79	2204	21.17	.69	2415	21.20	.60
1202	20.21	.44	1404	20.15	.56	2205	20.18	.58	2416	20.37	.53
1203	20.13	.54	1405	20.65	.65	2206	20.55	.52	2417	19.92	.58
1205	20.61	.49	1406	20.50	.55	2207	20.32	.62	2418	20.33	.59
1206	20.96	.86	1407	20.60	.54	2208	21.33	.60	2419	21.05	.77
1207	20.51	.61	1408	19.97	.52	2209	20.80	.54	2420	20.92	.56
1212	20.49	.53	1409	19.89	.30	2210	19.71	.52	2421	20.99	.56
1213	19.66	.53	1410	20.77	.48	2211	20.31	.55	2422	16.35	.53
1214	19.88	.53	1411	20.16	.41	2212	21.01	.68	2423	19.76	.78
1215	21.19	.91	1412	20.42	.51	2213	20.66	.59	2424	20.27	.56
1216	20.95	.58	1413	19.82	.51	2214	20.22	.55	2425	20.78	.67
1217	19.24	.65	1414	19.48	.49	2215	20.95	.64	2426	21.08	.57
1218	17.15	.71	1416	20.41	.48	2216	20.12	.61	2427	20.34	.50
1219	17.64	.84	1418	19.57	.77	2217	19.66	.45	2428	21.38	.78
1220	19.72	.63	1419	18.79	.65	2219	21.07	.66	2429	21.31	.71
1221	20.12	.45	1421	19.63	.39	2220	19.83	.56	2430	20.50	.59
1222	18.44	.64	1422	20.19	.45	2221	20.67	.52	2431	21.57	.74
1223	17.99	.84	1424	20.67	.74	2222	19.54	.81	2432	20.52	.54
1224	17.13	.74	1426	20.30	.58	2223	20.62	.58	3101	20.55	.44
1225	20.48	.61	1427	21.02	.65	2224	17.63	.90	3102	21.41	.64
1226	19.54	.49	1428	19.80	.45	2301	20.81	.52	3103	20.01	.55
1227	20.51	.64	1432	19.71	.53	2302	19.89	.52	3104	20.54	.57
1229	21.28	.78	1433	21.41	.51	2303	20.89	.69	3105	20.84	.57
1230	20.26	.44	1437	20.39	.65	2304	21.31	.75	3106	21.04	.69
1231	21.55	.77	1438	20.89	.52	2305	17.22	.93	3107	20.24	.58
1233	19.99	.52	1439	20.12	.46	2306	19.95	.53	3108	21.60	.55
1234	20.06	.50	1440	21.59	.74	2307	20.65	.49	3109	19.80	.66
1235	20.45	.68	1441	20.71	.57	2308	21.23	.77	3110	19.86	.61
1236	18.85	.32	1442	20.23	.44	2309	21.46	.78	3111	17.16	.76

TABLE 4—*Continued*

STAR	V	B-V	STAR	V	B-V	STAR	V	B-V	STAR	V	B-V
3112	21.07	.60	3211	20.54	.64	3303	20.20	.48	3404	20.87	.68
3113	20.98	.60	3212	21.27	.52	3304	20.40	.53	3405	20.82	.61
3114	21.10	.70	3213	20.89	.61	3305	20.33	.56	3406	20.56	.52
3115	20.98	.51	3214	20.53	.68	3306	21.11	.70	3407	21.62	.57
3116	20.96	.71	3215	20.49	.62	3307	21.29	.62	3408	21.30	.62
3117	21.51	.81	3216	20.37	.47	3308	20.65	.51	3409	21.30	.61
3118	21.16	.56	3217	20.99	.70	3310	19.50	.44	3410	21.41	.73
3119	21.32	.55	3218	19.74	.62	3311	18.84	.52	3411	21.06	.65
3120	21.26	.71	3219	21.05	.73	3312	20.18	.55	3412	21.29	.70
3121	19.94	.44	3220	20.71	.61	3313	19.39	.55	3413	21.36	.67
3122	21.32	.54	3221	20.37	.58	3314	20.57	.64	3414	21.63	.84
3123	20.46	1.33	3222	20.10	.54	3315	20.97	.48	3415	20.57	.63
3124	21.73	.49	3223	20.79	.65	3316	20.61	.55	3416	20.06	.50
3125	21.25	.55	3224	19.95	.62	3317	20.41	.46	3417	21.66	.52
3126	17.32	.92	3225	21.23	.63	3318	20.96	.70	3418	21.66	.58
3127	17.93	.85	3226	20.76	.65	3319	20.96	.81	3419	20.67	.64
3128	21.21	.29	3227	20.13	.48	3320	20.96	.68	3420	21.00	.64
3129	20.89	.53	3228	20.43	.52	3321	20.31	.51	3421	21.48	.49
3130	21.17	.74	3229	21.51	.61	3322	19.03	.81	3422	20.11	.54
3131	20.63	.53	3230	20.68	.58	3323	21.15	.61	3423	21.41	.67
3132	19.97	.56	3231	20.90	.58	3324	20.93	.63	3424	19.79	.55
3133	19.61	.52	3232	20.66	.43	3325	19.48	.40	3425	20.68	.60
3134	21.13	.50	3233	21.14	.84	3326	20.04	.54	3426	21.22	.68
3135	20.55	.58	3234	20.16	.62	3327	19.61	.53	3427	21.27	.70
3136	19.14	.83	3235	19.94	.56	3328	17.17	.74	3428	21.39	.71
3137	21.05	.47	3236	20.93	.67	3329	19.76	.40	3429	21.47	.66
3138	20.20	.64	3237	21.16	.71	3330	19.04	.85	3430	20.62	.57
3139	20.38	.59	3238	21.23	.67	3331	21.19	.73	3431	21.03	.51
3140	20.37	.58	3239	20.64	.78	3332	21.56	.68	3432	21.51	.78
3141	19.26	.58	3240	21.31	.65	3333	20.91	.48	3434	21.49	.69
3142	19.07	.80	3241	20.54	.55	3334	20.32	.56	3435	18.72	.83
3143	21.31	.70	3242	20.74	.67	3335	21.12	.57	3436	19.94	.49
3144	21.19	.87	3243	20.90	.73	3336	21.92	.50	3437	21.02	.67
3145	19.85	.37	3244	20.68	.55	3337	21.46	.60	3438	21.07	.78
3146	21.38	.83	3245	19.85	.67	3338	21.40	.69	3439	19.35	.82
3147	20.79	.57	3246	20.70	.51	3339	21.28	.85	3440	20.75	.75
3148	18.36	.63	3247	20.73	.59	3340	21.01	.51	3441	19.73	.75
3149	20.14	.57	3248	20.14	.44	3341	20.57	.58	3442	19.30	.81
3150	21.50	.58	3249	18.39	1.19	3342	20.96	.68	3443	21.30	.72
3151	20.77	.51	3251	21.43	.76	3343	21.04	.74	3444	21.58	.76
3152	20.53	.90	3253	21.70	.73	3344	20.76	.59	3445	21.47	.62
3153	21.14	.64	3254	21.66	.53	3345	20.41	.55	3446	20.57	.66
3158	21.79	.72	3255	21.66	.94	3346	20.83	.92	3447	21.77	.80
3159	21.76	1.05	3257	21.98	.61	3347	20.78	.59	3448	21.04	.50
3160	22.03	.39	3259	22.06	.73	3348	21.40	.01	3449	21.17	.70
3161	21.67	.67	3260	21.77	.65	3349	21.16	.70	3450	21.14	.65
3165	21.78	1.06	3264	21.91	.69	3350	20.65	.54	3451	20.56	.53
3166	21.48	.72	3265	21.89	.85	3351	19.91	.57	3452	20.98	.54
3168	21.57	.86	3266	21.70	.85	3352	21.65	.91	3453	21.17	.72
3172	21.43	.64	3268	21.56	1.01	3353	21.57	.89	3454	21.13	.73
3201	21.16	.71	3269	21.46	.64	3354	21.50	.68	3455	21.26	.97
3202	21.08	.75	3270	17.85	1.26	3356	21.65	.68	3456	20.37	.55
3203	20.14	.54	3274	21.36	1.06	3359	21.42	1.04	3457	19.85	.62
3204	20.64	.46	3276	21.55	.77	3360	21.46	.59	3458	20.25	.21
3205	20.55	.46	3277	21.32	.71	3361	21.62	.74	3459	20.54	1.44
3206	20.70	.68	3278	21.79	.85	3362	21.74	.85	3460	16.69	.83
3207	20.97	.70	3279	21.56	.67	3363	21.81	.48	3461	21.17	.64
3208	20.97	.63	3280	21.56	.85	3401	21.15	.62	3463	21.76	.76
3209	21.12	.73	3301	19.15	.83	3402	20.83	.69	3464	21.59	.83
3210	21.48	.63	3302	21.09	.66	3403	19.96	.51	3465	21.39	.98

TABLE 4—*Continued*

STAR	V	B-V
3466	21.49	.76
3469	21.54	.84
3470	22.00	.56
3471	21.56	.86
3473	21.99	.76
3474	21.39	1.22
3475	21.97	.99
3476	21.65	.88
3481	21.86	.58
4101	18.22	.77
4102	20.76	.57
4103	18.81	.81
4104	17.27	.95
4105	21.09	.68
4106	21.46	.89
4107	20.32	.55
4108	19.93	.53
4109	21.15	.83
4110	20.89	.38
4111	20.96	.79
4112	20.50	.41
4113	21.22	.82
4114	20.38	.54
4115	20.22	1.12
4116	18.32	.77
4117	21.30	.91
4118	20.83	.40
4119	20.55	.47
4120	20.88	.57
4121	20.59	.49
4122	15.88	.83
4123	19.95	.65
4124	20.05	.60
4125	21.30	.84
4126	21.27	.75
4127	20.95	1.34
4128	21.43	.93
4129	21.35	.83
4130	21.05	1.39
4131	19.85	.50
4132	21.34	.88
4133	19.31	.81
4134	21.32	.57
4135	18.31	.94
4136	19.93	.53
4137	21.05	.84
4138	21.28	.95
4139	19.39	.79
4140	20.88	.63
4141	21.29	.76
4143	20.73	.69
4144	20.17	1.76
4145	21.34	.86
4146	19.59	.84
4147	20.42	1.35
4148	20.67	1.42
4149	20.06	1.28
4150	21.09	.76
4151	21.42	.75
4152	20.61	.51
4153	21.22	.90
4154	16.51	1.50
4155	20.13	.46
4156	19.59	.55
4157	19.42	.77
4158	20.30	.77
4159	21.47	.96
4201	20.97	.77
4202	20.90	.67
4203	21.31	.91
4204	21.24	1.19
4205	21.43	1.03
4206	21.12	.46
4207	20.66	.74
4208	21.23	.74
4209	21.31	1.32
4210	16.32	1.02
4211	19.80	.67
4212	20.94	.68
4213	18.69	.74
4214	20.58	1.42
4215	19.11	.92
4216	21.10	.84
4217	19.35	.83
4218	20.94	.78
4219	21.11	.79
4220	19.43	.75
4221	20.72	.81
4222	20.70	.58
4223	19.46	.50
4224	21.03	.81
4226	18.57	.84
4227	20.32	1.61
4228	19.27	.53
4229	21.02	1.15
4230	21.01	.79
4231	20.07	.51
4232	17.42	.72
4233	21.31	1.12
4234	16.73	.56
4235	20.62	.69
4236	20.18	.49
4237	20.98	.74
4238	20.74	.60
4239	20.80	.68
4240	20.97	.79
4241	19.95	1.50
4242	21.09	.76
4243	21.01	.75
4244	20.57	.53
4245	15.32	1.27
4301	20.03	.62
4302	20.47	.62
4303	20.21	.59
4304	20.20	.42
4305	20.87	.80
4307	20.01	.60
4308	20.64	.56
4309	19.11	1.53
4310	20.54	.56
4311	19.83	.70
4312	20.61	.48
4313	20.98	.68
4314	20.79	1.53
4315	20.56	.61
4316	21.01	.80
4317	20.44	1.51
4318	21.20	.72
4319	18.93	1.45
4320	21.17	.82
4321	19.59	.92
4322	20.65	.53
4323	16.74	.64
4324	19.83	.54
4325	20.70	1.59
4326	21.07	1.20
4327	19.42	1.17
4328	20.48	.55
4329	19.84	.61
4330	16.21	.40
4331	21.54	1.01
4332	20.69	.65
4333	19.89	.56
4334	20.07	.54
4335	16.06	1.45
4336	18.09	.84
4337	20.93	.61
4338	20.50	.57
4339	18.63	.62
4340	21.32	.75
4341	21.19	.65
4342	21.32	.70
4343	20.33	.51
4344	20.87	.65
4345	20.76	1.28
4346	21.20	1.18
4347	20.55	.40
4348	20.50	1.63
4349	20.07	.48
4350	20.18	.46
4351	20.11	1.23
4352	21.03	.57
4353	21.24	.70
4354	20.49	.72
4401	20.86	.71
4402	21.09	.65
4403	20.68	.44
4404	19.67	.44
4405	21.18	.72
4406	20.80	.43
4407	21.14	.81
4408	21.19	.95
4409	21.19	.79
4410	20.41	1.39
4411	20.73	1.40
4412	21.18	.64
4413	21.23	.92
4414	19.30	1.45
4415	21.21	.55
4416	21.31	.89
4417	20.58	.50
4418	19.45	.48
4419	20.22	.52
4420	21.25	.97
4421	21.63	.99
4422	15.52	.64
4423	20.71	.50
4424	19.92	.51
4425	21.17	.69
4426	21.42	.95
4427	19.40	.49
4428	20.89	.80
4429	21.15	.97
4430	21.26	.75
4431	15.72	.90
4432	17.80	.96
4433	21.05	.58
4434	16.97	1.10
4435	16.36	.53
4436	19.43	1.32
4437	20.95	−.08
4438	19.96	1.49
4439	21.10	.62
4440	21.14	.71
4441	20.95	.91
4442	21.08	.89
4443	20.66	1.47
4444	20.67	1.53
4445	19.54	1.51
4446	20.48	.64
4447	20.58	.41
4448	15.96	1.06
4449	20.84	.61
4450	21.13	.80
4451	19.51	1.46
4452	21.24	.73
4453	21.21	.83
4454	21.12	.66
4455	19.09	.72
4456	16.60	.77

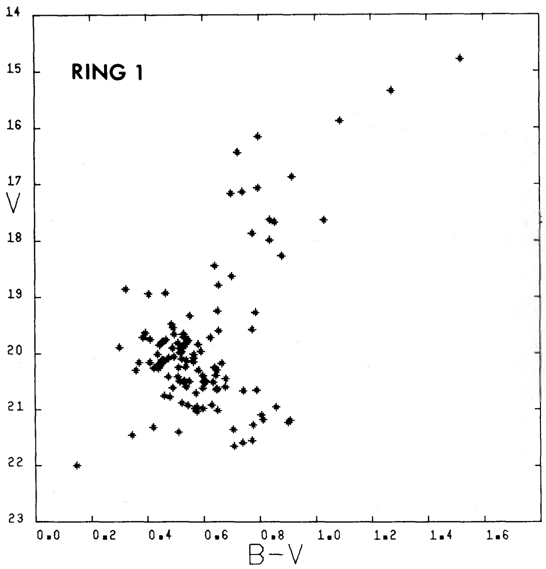

FIG. 6a

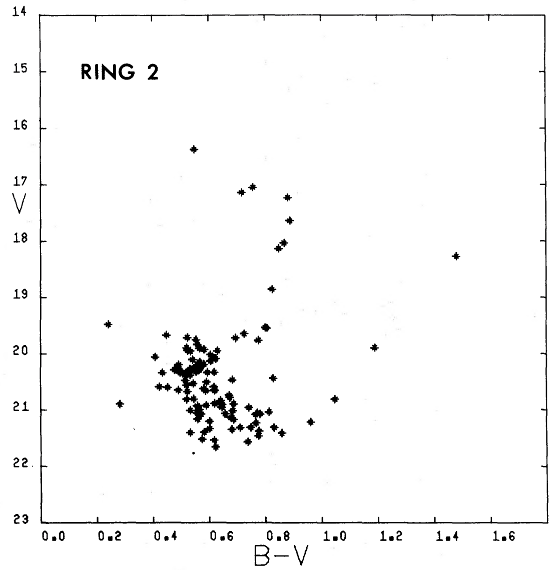

FIG. 6b

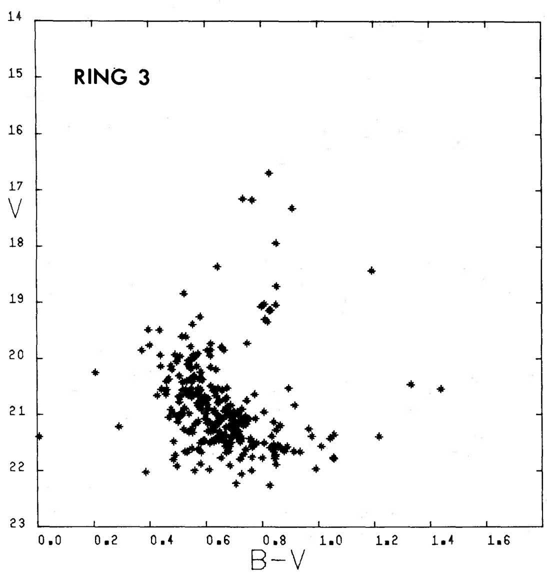

FIG. 6c

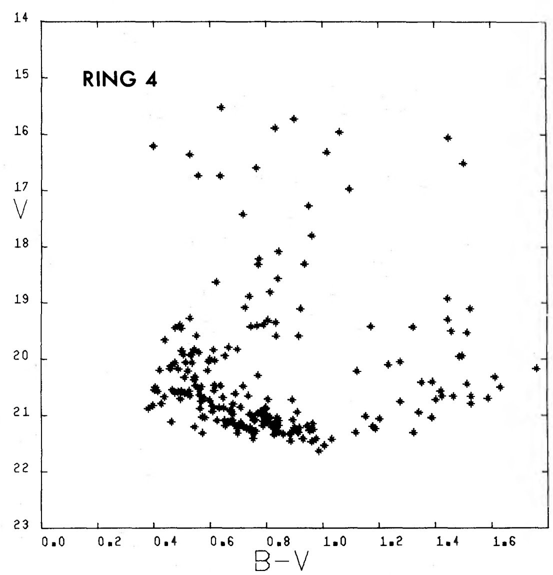

FIG. 6d

FIG. 6a–d.—Color-magnitude diagrams for the individual rings 1–4. These results are from the 4 m plates only; the final data for the bright ($V < 19$) stars differ slightly from these diagrams since the 1.5 m plates are averaged in.

to 22 for rings 2 and 3) than in the more open outer regions. Most of the star images fainter than $V \sim 20$ in ring 1 either crowd each other noticeably or lie on a slightly higher background density, so the photometry could not be pushed deeper with safety. The plates from the 1.5 m, which had brighter limits than the 4 m plates by ~2 mag and were thus virtually free from crowding problems, were used primarily to correct the photometry for the brighter stars ($V \lesssim 19$), especially in ring 1.

To delineate the entire cluster more clearly, we formed a composite CMD comprising all stars in rings 2 and 3, *plus* stars brighter than $V = 19$ in ring 1. The result is in Figure 7, and the mean lines for the CMD sequences are listed in Table 5.[4]

In general, the CMD morphology of Pal 12 resembles that of the prototype "metal-rich" cluster 47 Tuc (Hesser and Hartwick 1977). Several specific features of Figures 6 and 7 are notable:

1) The HB—which is clearly seen only in the

[4] The composite diagram of Figure 7 completely supersedes a preliminary version we presented earlier (Harris and Canterna 1978). The small systematic differences between the two versions, and hence in the derived physical properties of the cluster, result mainly from a greatly improved plate-to-plate reduction in the present work.

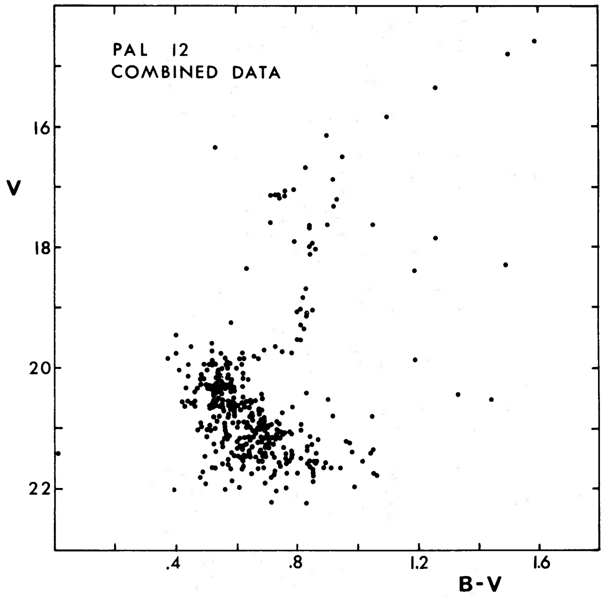

FIG. 7.—Composite CMD for Pal 12, including all stars from rings 2 and 3 plus brighter ($V < 19$) stars from ring 1. This diagram best shows the principal sequences of the cluster.

composite diagram—is evidently a degenerate "red stub" of seven to eight stars at $V = 17.1$, $B - V = 0.75$. No blue HB stars or RR Lyrae variables are noticeable anywhere. The color range spanned by the HB is only $\Delta(B - V) = 0.04$, and within the errors of measurement its stars are photometrically virtually identical; in this respect Pal 12 more nearly resembles old *open* clusters such as M67 (Racine 1971) or NGC 2420 (McClure, Forrester, and Gibson 1974) than most red globular clusters.

2) The cluster stars above the HB form a surprisingly well-marked sequence of only six to seven red giants, and (perhaps) two asymptotic-branch stars above the red end of the HB. The giant branch (GB) itself is parametrized by a slope S (Hartwick 1968) of 3.7, a height ΔV (Sandage and Wallerstein 1960) of 2.20, and a base color $(B - V)_{0,g}$ (Sandage and Smith 1966) of 0.89. All three of these parameters as well as the red HB are indicative of relatively high heavy-element abundance, similar to the prototype of this class, 47 Tuc (cf. Hesser and Hartwick 1977).

3) The different rings contain noticeably different proportions of bright and faint cluster stars. Further comments on this radial dependence of the cluster luminosity function will be made in § VI.

4) The main-sequence turnoff point (where $B - V$ is a minimum) appears at $V_{\text{to}} = 20.3 \pm 0.2$, $(B - V)_{\text{to}} = 0.54 \pm 0.03$ and the magnitude difference between HB and turnoff is then $V_{\text{to-HB}} = 3.2 \pm 0.2$. This value is quite similar to corresponding numbers from other globular clusters with well-defined main sequences (Sandage 1970; Hesser and Hartwick 1977) and suggests immediately that Pal 12 must be at least roughly the same age as other globular clusters. (The HB luminosity decreases more slowly with time than does the turnoff, but the abundance effects on each are similar, so $V_{\text{to-HB}}$ is primarily a function of age; cf. Hartwick and Vanden Berg 1973; Iben 1971; Sweigart and Gross 1976.) The magnitude difference $V_{\text{to-HB}}$ also acts as a (weak) consistency check on the adopted value of $\Delta m = 6.8$ for the secondary-image calibration, since the determination of V_{HB} relies only on the primary photoelectric standards, while V_{to} relies instead on the secondary image standards.

The general scatter in $B - V$ of the points in Figure 7 increases markedly just at the turnoff, $V \sim 20$. This is due not only to the general increase of random error with magnitude but also to the smaller number of plates used. The main-sequence photometry relies on only the three deepest plates in each color, whereas from the base of the giant branch upward, all 16 plates (Table 3) could be used.

5) In Figure 7, half-a-dozen stars are seen to stand off the upper left of the turnoff (around $V = 19.9$, $B - V = 0.43$) and can properly be called blue stragglers. Most of them are from ring 3. None of their images on the photographic plates appear crowded or asymmetric, they are obviously well above the plate limit, and we can find no reasons to doubt the photometry at the level of $\Delta(B - V) \lesssim 0.05$ mag. If their locations are valid, Pal 12 would join M3 (Sandage 1970) and possibly NGC 6352 (Hartwick and Hesser 1972) and M71 (Arp and Hartwick 1971) in the small group of globular clusters believed to contain blue stragglers. If they are single stars in the normal course of evolution (which we believe unlikely), then the isochrone fits discussed in § VII below would imply they must be at most 5–6 × 10^9 years old, less than half the best estimate of the cluster age itself. Other working hypotheses for blue stragglers which invoke binary mass transfer or delayed evolution are well known and need not be reviewed here (see McCrea 1964; Strom, Strom, and Bregman 1971; Carney and Peterson 1979; Carney 1979; Wheeler 1979).

6) In ring 4 a group of stars attached to the lower right of the main sequence ($V > 21$, $B - V \approx 0.8$) appears which is not present in the other rings. Instead

TABLE 5

MEAN LINES FOR PAL 12 COLOR-MAGNITUDE DIAGRAM

V	$B - V$	V	$B - V$
14.60	1.60	19.00	0.82
15.00	1.40	19.60	0.80
15.55	1.20	19.75	0.70
15.85	1.10	19.82	0.60
16.32	1.00	20.00	0.55
17.15	0.90	20.30	0.54
18.00	0.85	20.75	0.60
18.50	0.83	21.50	0.70
Horizontal Branch			
17.05	0.79	17.15	0.71

of being field stars, we believe these are likely to be the faint extension of the main sequence, shifted over by small photographic errors near the limit. Selective removals of individual plates or realistic variations in the reduction parameters did not affect their position strongly, but ring 4 was measured and reduced separately from the others and so different results near the limit are quite possible. We are unable to make any further judgments without a more thorough photometric calibration below V ~ 21 than we have at present.

7) From inspection of magnitude residuals on our total of eight plates in each color we were able to find no definite variable stars in this study, and it appears most likely that the cluster has none. Three stars were proposed by Kinman and Rosino (1962) as cluster variables: of these, their stars 1 and 2 are our 4112 and 4118, and their star 3 was too faint to be measured reliably here. On our plates of best seeing, all three appear to be at least slightly nonstellar, and there are many other faint galaxy images in the same region. Variable 3 is particularly notable since, according to Kinman and Rosino, it appears near the detection limit ($B \sim 22$) on all 16 of their plates *except* one, where it was at $B \sim 18.5$. At its position there is an almost undetectable galaxy image on our plates, and thus the variable may simply have been a supernova in the extremely distant galaxy that we now see there. In any case, the Kinman-Rosino stars are much too faint to be considered possible cluster variables (even the first two showed no especially large residuals and are below $V = 20$).

IV. FOREGROUND REDDENING AND DISTANCE

The galactic foreground reddening of Pal 12 can be estimated (*independently* of any properties of the cluster itself which are under discussion here), either from the color-color relation for the foreground field stars or from the cosecant law. In Figure 8 the $(U - B, B - V)$ diagram for the photoelectric standards of Table 1 is shown. Allowing for the obvious presence of metal-poor giants and subdwarfs at this high latitude, we obtain a simple upper limit of $E_{B-V} \lesssim 0.03$. The cosecant law (cf. Harris 1976 and references cited) for globular clusters yields a value of 0.02 ± 0.02. The two estimates are consistent, and we adopt $E_{B-V} = 0.02$ for the following discussion. *Because the cluster reddening is essentially negligible*, our conclusions concerning the various physical properties of Pal 12 (age, distance, abundances, etc.) cannot be seriously affected by uncertainties in absorption corrections alone.

The distance may be estimated by using $M_V(\mathrm{HB}) = 0.9 \pm 0.3$ from the main-sequence fit (§ VII), which then gives $(m - M)_V = 16.2 \pm 0.35$. With $A_V/E_{B-V} = 3.2$ we obtain a true distance of 17 kpc from the Sun, and $R_{GC} = 14$ kpc from the galactic center if $R_\odot = 9$ kpc (Harris 1976). This measurement of distance directly from the CMD is smaller by factors of 2 or more than previous estimates (e.g., Arp 1965; Harris 1976). The two reasons for this large discrepancy are,

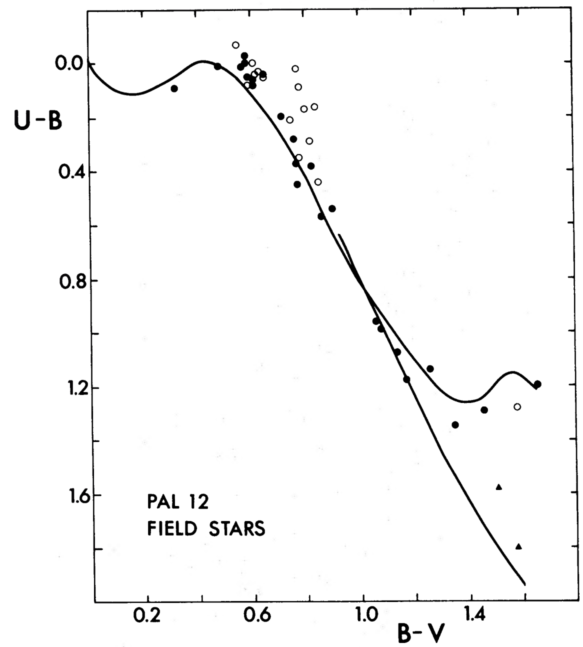

FIG. 8.—Two-color diagram for the photoelectric standard stars. Filled circles are bright standards ($V < 14$), open circles fainter ones, and triangles are the two red giants believed to be members of Pal 12. The intrinsic unreddened lines for luminosity classes V and III (Fitzgerald 1969) are drawn in.

first, that the use of the old 25 brightest stars method was invalid since (as is now clear) Pal 12 has only a handful of bright giants; and second, the three faint Kinman-Rosino "variables" were assumed to be RR Lyrae members. Both caused significant overestimates of the cluster distance. Comparable errors in current distance estimates for other outlying clusters without CMD's are entirely possible.

V. ABUNDANCE PARAMETERS

Aside from the CMD itself (§ VII below), we are able to obtain information on the chemical composition of the Pal 12 stars in several ways at various levels of sophistication:

1) The ultraviolet excess $\delta(U - B)$ for two cluster giants (stars 1 and 2 in Table 1) is $+0.16$, which is similar to $\delta(U - B)$ for the giants in clusters of intermediate or moderately high metallicity such as M3, M13, or even 47 Tuc. Because of the crude nature of $\delta(U - B)$, by this method we can obtain only a very rough estimate $[\mathrm{Fe/H}] \sim -1.5$.

2) Spectra of the same stars 1 and 2 have been taken by Cowley, Hartwick, and Sargent (1978). Their abundance indices, based on a combination of the metallic line strengths between Hδ and the Ca II H line, the Mg *b* lines at $\lambda 5180$, and the H and K lines, also suggest a moderately low [Fe/H], though more metal-rich than M92 or M15. But no precise estimates are possible here either, since their grid of "standard"

clusters is not extensive. Their spectra suggest in addition that the CN band strengths are enhanced, similar to the "CN-strong" giants in NGC 7006, and that the CH-band strengths are higher than in NGC 7006.

3) Canterna and Schommer (1978) measured the four brightest cluster giants with the CMT_1T_2 broad-band photometric system. Their average [Fe/H] over all four stars is -1.2 ± 0.5 but is highly uncertain because the individual measured values run from 0.0 to -2.5. (The mean [Fe/H] $= -1.7$ which Canterna and Schommer actually quote [see their Table 2] was obtained from only the three lowest values; but there seems to be no reason at present to exclude any of them since all four are equally likely to be members from the C-M diagram.) Three of the giants in their list also show evidence for enhanced CN and/or CH, though the Washington system cannot distinguish between these two features. However, it is clear that none of the data in points (1)–(3) above provide much critically useful information on the composition of Pal 12 except to say that it is probably not extremely metal-poor and that there is some hint of $Z_{\rm CNO}$ enrichment.

4) Cohen *et al.* (1980) have recently reported, from infrared CO-band photometry and optical spectroscopy of the same four Canterna-Schommer stars, that the Pal 12 giants are closely similar to those in M71, in both overall metal-line strength and CO band strength. This work provides the first definitive evidence that Pal 12 in fact belongs toward the upper end of the metallicity scale for globular clusters.

5) Most recently (1979 October) we have obtained a large new collection of CTIO vidicon spectra (resolution 3 Å per pixel) for giants in several globular clusters covering the metallicity range from M15 up to 47 Tuc. Though full results will be described elsewhere, for six Pal 12 stars in the set we find (*a*) their Ca line strengths place Pal 12 noticeably but slightly (≈ 0.2 dex) on the metal-poor side of 47 Tuc, and (*b*) the ultraviolet ($\lambda 3880$) CN band strengths are virtually identical with those in 47 Tuc, as is the CH band.

The newer and more detailed spectroscopic data summarized in points (4) and (5) take precedence over the previous approximate indicators, and rather than assigning Pal 12 to the "anomalous" class of outer-halo objects as we had originally anticipated, we must place it in with the more familiar "metal-rich" group of globular clusters. But it remains an intriguing object for quite different reasons: at 14 kpc from the galactic center it is easily the most distant of all the clusters in its abundance group.

The actual [Fe/H] value for Pal 12 must then be specified by analogy with the prototypes 47 Tuc or M71. The recent and important high-dispersion composition analyses of Cohen (1979) and Pilachowski (1979) yield [Fe/H] $= -1.2$ for M71 and 47 Tuc. In addition, they find significant enhancement of oxygen, [O/Fe] $\sim +0.5$, in both these standard clusters. Although no direct measurement of [O/H] for Pal 12 itself is available yet, we suspect from the combined weight of evidence discussed above, and from its established similarity with M71 and 47 Tuc, that the same relative CNO enrichment will turn out to hold for Pal 12 as well. The main-sequence isochrone fit (§ VII below) gives additional indirect support to this view. The decoupling of $Z_{\rm CNO}$ from $Z_{\rm Fe}$ for the "metal-rich" globular clusters presents a compelling new problem in understanding the nucleosynthesis history of the halo. A strongly related argument appears to be in the recent abundance work on field halo *stars* by Sneden, Lambert, and Whitaker (1979). They find that [O/Fe] is essentially zero for stars with [Fe/H] $\gtrsim -0.5$, but that in the range $-0.5 <$ [Fe/H] < -2.0, [O/Fe] jumps to a roughly constant value of $+0.5$, in agreement with the new globular cluster analyses. These combined results already suggest that the halo is chemically much more distinct from the oldest parts of the disk (including the oldest and most metal-poor known open clusters) than was previously realized. Some implications of this on the main-sequence fitting and age determination of Pal 12 will be discussed below.

VI. LUMINOSITY FUNCTION AND INTEGRATED PROPERTIES

Because the C-M data in Pal 12 cover such a wide magnitude range, it is possible to investigate the cluster luminosity function $\phi(M_V)$. The basic questions as to how ϕ (and hence stellar mass distribution) is affected by such integrated cluster properties as total population, central concentration, or metallicity are still largely unanswered, particularly for the faint main sequence, so the present data for Pal 12 may eventually contribute to such studies.

Even a casual inspection of the CMDs in Figure 6 hints that an interesting radial trend exists in the luminosity distribution of cluster members. Almost all the red giants above the HB lie in ring 1; rings 2 and 3 contain almost nothing but main-sequence and subgiant stars; while in ring 4 nothing easily distinguishable from the spread of field stars can be seen except for the main-sequence turnoff. (Incidentally, it is plain that virtually all the bright stars ($14 < V < 18$) in rings 1–3 must be cluster members. Even if we assume all such stars in ring 4 are field objects, and scale their numbers down by the ratios of ring areas, we conclude that at *most* one such field star should lie in each of rings 1 and 2, and five in ring 3. Thus, it seems necessary to accept the thin extension of the giant branch to the upper right corner in Figures 6*a* and 7 as being a real feature of the cluster.)

Despite the small total numbers of cluster stars, the outward trend of progressively losing the bright giants appears significant. Using the cluster structural parameters (see below), we find that ring 1 alone contains only 25% of the total cluster light (and indeed only 10% of the total surface area for rings 1–3), yet it also has six of the eight red giants above the HB. Applying conventional χ^2 or small-number statistical tests suggests that this is not due to chance at more than 95% confidence. In addition, the ratio of the number of subgiant and turnoff stars seen in Figure 6 (i.e., stars in the interval $19.5 < V < 20.2$) to cluster giants ($V < 19$) increases from ~ 4 in ring 1 to ~ 5 in ring 2, ~ 10 in ring 3, and $\gtrsim 15$ in ring 4. (Similar effects are seen if the main-sequence stars ($20 < V < 21$) are compared with the giants, though the photometry becomes progressively more incomplete for them.) Because the main sequence is so much more heavily populated than the giant branch to begin with, this ratio will be a sensitive function of any real radial changes in their relative numbers.

The first explanation that might logically be suggested for this radial stratification of the different types of stars would be dynamical relaxation, since the central relaxation time for Pal 12 as calculated by the method of Peterson and King (1975) is $\sim 10^9$ years, and stellar lifetimes along the giant branch are comparably long. In this case the giants evolving up the Hayashi line would have to be more massive than the main-sequence stars below the turnoff, in order to sink toward the cluster center over a few relaxation times. But the actual expected mass difference between turnoff and giant-branch tip is believed on theoretical grounds to be small ($\lesssim 0.05\ M_\odot$; see Ciardullo and Demarque 1977), and it is therefore hard to see how the relaxation process could be effective enough. We are unable to suggest any other very natural mechanisms to produce the observed effect but can only suggest that similar effects be searched for in other globular clusters of relatively open or sparse structure (e.g., NGC 5053, NGC 6809, Pal 5, or even ω Cen). It is worth stressing that Pal 12 provides a rare chance to evaluate these radial trends in the luminosity function, since the entire CMD down to the main sequence is measurable at *every* radius. In the great majority of globular clusters, the main sequence is unobservable in the cluster center because of either distance or prohibitive crowding, and any conclusions about stellar population trends with radius have had to rely only on subsets of the bright stars (giant or HB) or on the application of theoretical structural models (e.g., Woolf 1964; Dickens and Rolland 1972; Da Costa and Freeman 1976; Spitzer and Shull 1975; Gunn and Griffin 1979; Angeletti and Giannone 1979). Thus Pal 12 is particularly useful in demonstrating the effects of stellar dynamical processes on the stellar distribution within the cluster, due to the very characteristics which make it otherwise undistinguished.

In Table 6 we list the cumulative luminosity function in each ring (rings 2 and 3 are arbitrarily combined since little difference appears between them). N is the total number of stars brighter than magnitude V; the last column is a normalized sum over rings 1–3 to provide an approximate "average" luminosity function for rough comparison with other clusters. We constructed this last column as the direct sum of rings 1–3 for $V < 20.2$, and for $V \geq 20.4$ as the sum of rings 2 and 3 (multiplied by the scale factor of 1.78 to match up the total at $V = 20.2$). This approach was used since for $V \gtrsim 20$, the totals in ring 1 become significantly incomplete (approximately one-third of all the faint stars in ring 1 were too crowded to be measured, as can be seen from inspection of Figure 3). Hence only rings 2 and 3 were adopted as representing a valid total for the fainter stars; ring 4 is, of course, heavily contaminated with field stars at all magnitudes and was not used.

In Figure 9 the differential luminosity function ϕ is plotted, as derived from the normalized total function $N(V)$ in Table 6. Before plotting ϕ(solid-line histogram in Fig. 9), it was approximately corrected for field stars by using ring 4: we assumed all ring 4 stars for $V \leq 19$ to be field stars and half of them for $V \geq 19$. After compensating for the relative ring areas, these field-star totals were subtracted from rings 1–3. In practice,

TABLE 6

Luminosity Function Data

V	$N(\leq V)$ By Ring: 1	2 + 3	4	Normalized[a] Total
14.6	0	1	1	1
14.8	1	1	1	2
15.0	1	1	1	2
15.2	1	1	1	2
15.4	2	1	2	3
15.6	2	1	3	3
15.8	2	1	4	3
16.0	3	1	6	4
16.2	4	1	8	5
16.4	4	2	11	6
16.6	5	2	14	7
16.8	5	3	16	8
17.0	6	3	17	9
17.2	9	7	17	16
17.4	9	9	18	18
17.6	9	9	19	18
17.8	12	11	20	23
18.0	14	13	21	27
18.2	14	15	22	29
18.4	15	17	25	32
18.6	16	17	26	33
18.8	18	18	27	36
19.0	21	20	30	41
19.2	21	25	33	46
19.4	24	29	39	53
19.6	28	33	50	61
19.8	40	46	52	86
20.0	50	63	63	113
20.2	65	83	76	148
20.4	77	108	84	193
20.6	90	135	103	241
20.8	99	166	126	296
21.0	106	202	147	360
21.2	111	248	181	442
21.4	115	286	207	510
21.6	119	319	214	569
21.8	120	343	215	612
22.0	120	352		628
22.2	120	354		631

[a] Equals direct sum of rings 1–3 for $V \leq 20.2$; after that, rings 2 + 3 multiplied by normalization factor 1.78 to account for ring 1 incompleteness. See text. No corrections are made for field stars.

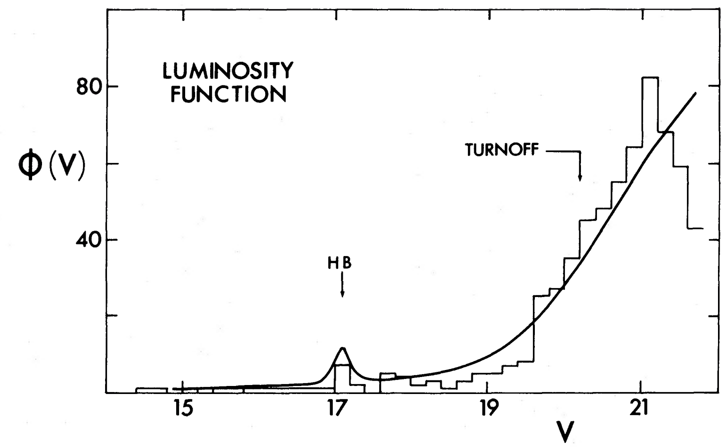

FIG. 9.—Luminosity function for Pal 12. Here $\phi(V)$ is the number of cluster stars found in each 0.2 mag bin as shown. Rings 1, 2, and 3 were used as described in the text to form the $\phi(V)$ data. Magnitude levels of the HB and the turnoff (bluest point on the main sequence) are indicated. The smooth line drawn over the histogram for Pal 12 is the M3 function (Sandage 1957) scaled down by a factor of 35, normalized arbitrarily to 440 stars brighter than $V = 21.2$.

since the inner rings have so much smaller area, this correction turned out to be small enough to be almost negligible at all levels.

The mean $\phi(M_V)$ curve for the classic cluster M3 (Sandage 1957) is added in Figure 9 for comparison, arbitrarily reduced by a factor of 35 to match the Pal 12 total $N(21.2) = 440$. The slight differences in shape between the Pal 12 and M3 curves (in particular, the apparent deficiency of bright giants in Pal 12, or relative excess of main-sequence stars) are probably not significant considering that in both clusters the luminosity functions were derived by combining bright stars from the inner radial regions with faint ones from regions farther out. This procedure is strictly not correct since it obscures any intrinsic dependence of ϕ on radius, as discussed above; and without knowing the radial effects of dynamical relaxation to begin with it is not clear how an average $\phi(V)$ over all radii may be skewed. The main conclusion from Figure 9 is that the luminosity function of Pal 12 does not differ in any major way from "standard" globular clusters down to the limit of our survey ($M_V \sim +5$).

For most globular clusters the most efficient way to obtain *integrated* colors and luminosities is through direct photoelectric aperture photometry. By contrast, the Palomar clusters are so sparse that it is preferable to add up the individual stars. Combining all stars in rings 1–3 (excluding the few which lie far off the principal sequences), we obtain a total visual magnitude $V = 12.54$ and color $B - V = 0.90$.

Extrapolating these totals outward to include the entire cluster first requires knowing the structural parameters of the system. From star counts out to $r = 20'$ on our two deepest plates, we determine "core" and "tidal" radii (Peterson and King 1975) of $r_c \approx 1'.1 \pm 0'.3$, $r_t = 7'.5 \pm 1'.0$, with $\log(r_t/r_c) = 0.90 \pm 0.2$. An independent study by Peterson (1976) gave $r_t \approx 10'.7$ for Pal 12 from one Hale 200 inch plate. Given the many uncertainties involved in star counting, the difference does not appear serious to us, but we will adopt our own result since our counts went out further than Peterson's (20′ as opposed to 16′), and we believe the field subtraction to be better determined. With $r_t = 7'.5$ and the King (1966) structural curves, the outer radius of ring 3 should then contain $\sim 73\%$ of the total cluster. Correcting for this and adding a further (nearly negligible) 3% to compensate for the unobserved stars fainter than $V = 22$ (Sandage 1957), we finally calculate an integrated cluster magnitude of $V_t = 12.27$. Both V_t and $B - V$ compare satisfactorily with the directly observed values of $V \approx 12.42$, $B - V \approx 0.88$ by Racine (1975), measured photoelectrically through a $1'.6$ diameter aperture.

With our adopted distance modulus and reddening, the intrinsic luminosity and color of Pal 12 are $M_V \approx -4.0$, $(B - V)_0 = 0.88$. The integrated color is similar to the colors of usual "metal-rich" globular clusters [e.g., $(B - V)_0 = 0.85$ for 47 Tuc] and further strengthens the classification of Pal 12 as one of them. The absolute integrated magnitude of -4.0 makes Pal 12 the second least populous globular cluster known, after Pal 13 (see Harris and Racine 1979). With $M/L \sim 1.5$ (Illingworth 1976), the luminosity of Pal 12 corresponds to a total cluster mass of $\sim 5200\ M_\odot$, hardly bigger than many open clusters. It is also interesting that the directly observed figure $M_{V_t} \approx -4.0$ compares poorly with the value $M_{V_t} = -4.8$ which we would obtain by reducing the luminosity of M3 by the same factor of 35 used in Figure 9; however, this discrepancy is almost entirely due to the artifact of the relative "giant-poor" nature of Pal 12 compared with the standard M3 function as mentioned earlier. If we had normalized the M3 curve to only the *giant* branch of Pal 12 (e.g., for $V \lesssim 19.5$), then the reduction factor would have been ~ 60 instead of 35. Since the giants dominate the integrated light, the discrepancy between the measured magnitude and that predicted from the scaled M3 luminosity function is completely removed.

More generally, it would appear risky to rely on intercomparisons of cluster luminosity functions *alone* to derive accurate integrated magnitudes, especially for the sparse clusters with small numbers of giants.

Knowing the tidal radius and mass of Pal 12 enables an approximate estimate of its perigalactic distance R_p to be made. With $R_p \approx r_t\,(3.5\,M_{gal}/M_{cl})^{1/3}$ (e.g., King 1962) and $M_{gal} \sim 10^{11}\,M_\odot$, we obtain $R_p \approx 15$ kpc. Within the uncertainties this is identical with its present galactocentric distance of 14 kpc, and implies that we are *now* observing Pal 12 near its perigalactic point. If Pal 12 is indeed a "metal-rich" cluster, it must therefore stay considerably farther from the Galactic center than any other such clusters, which are generally within $R_{GC} \sim 8$ kpc (Harris 1976; Harris and Racine 1979). Unless the orbit of Pal 12 happens to be nearly circular, it must in fact spend most of its time even farther out in the halo. It now marks the upper limit of metallicities found among the globular clusters in the halo region 10 kpc $< R_{GC} <$ 20 kpc; and the range of metallicities found in this region is therefore significantly greater than has previously been realized (cf. Searle and Zinn 1978; Harris and Canterna 1979).

VII. MAIN-SEQUENCE FITTING AND AGE

Reliable age determinations for globular clusters, by direct fits of the observed main-sequence turnoff region to theoretical isochrones, are currently possible for only a small number of well-studied objects. Most age determinations of these few clusters (e.g., Sandage 1970; Hartwick and Hesser 1974; Böhm-Vitense and Szkody 1973; Demarque and McClure 1977) have yielded similar ages for all of them within the internal errors of fitting and have led to the traditional viewpoint that the epoch of halo formation must have been sharply defined, lasting perhaps $\sim 2 \times 10^9$ years or less (e.g., Eggen, Lynden-Bell, and Sandage 1962; Searle and Zinn 1978). But some other recent discussions (Saio 1977; Carney 1980) have advocated a much longer cluster formation period, lasting perhaps up to half the age of the Galaxy even in the vicinity of the Sun, such that the most metal-poor clusters formed earliest. The formation models for disk galaxies by Larson (1976) suggest also that particularly the outer parts of the halo may take several billion years to complete their star-formation period, though the models do not suggest quite as extensive a period as is proposed by Carney (1979). The more specific possibility of interpreting the strongly anomalous halo systems (Palomar clusters and dwarf spheroidals) as "young" Population II objects has also been advanced in several papers (see references cited in § I).

For Pal 12 the main sequence is now clearly enough defined that its age can be estimated. To carry this out we have adopted the basic approach of Demarque and McClure (1977), which is to transform the theoretical isochrones (M_{bol} versus $\log T_{eff}$) into the observational plane (M_V versus $B - V$) and then to compare the translated isochrones directly with the CMD. We used the recently published Yale isochrones (Ciardullo and Demarque 1977; Demarque 1978), which provide the largest available homogeneous set of models and cover the necessary abundance and age ranges.

The best-fitting set of isochrone parameters that we could achieve is displayed in Figure 10. The model composition is $Y = 0.20$, $Z = 0.004$ ([Fe/H] $= -0.7$), the cluster age is seen to be $(11 \pm 2) \times 10^9$ years, and the luminosity of the horizontal branch is set at $M_V(\mathrm{HB}) = 0.9$. The quality of fit relies entirely on (*a*) the lower–main-sequence positioning, combined with (*b*) the color and luminosity level of the turnoff, and (*c*) the luminosity and horizontal slope of the *subgiant* branch (i.e., the portion of the track between the turnoff and the base of the red-giant branch). The fit of the model giant branch (Hayashi track) to the observations is, of course, irrelevant since its temperature can be adjusted arbitrarily by varying the model convective mixing-length parameter l/H. (The main sequence is relatively unaffected by changes in l/H. The isochrones in Figure 10 are from models with $l/H = 1.6$ as transmitted to us by Demarque [1978], but use of the corresponding models with $l/H = 1.0$ resulted in no differences in our conclusions to well within the errors of fit.)

It will also be noticed from Figure 10 that the slope of the observed lower main sequence in Pal 12 is shallower than that of the isochrone ZAMS, so that the majority of the faintest main-sequence stars ($V > 21$) lie to the right of the isochrone line. Quite similar effects can be seen in isochrone fits to other globular clusters (see, e.g., Carney 1980), and we

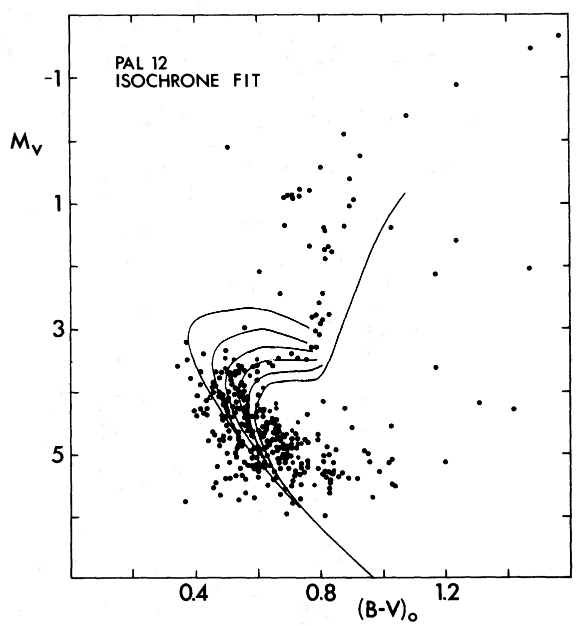

FIG. 10.—Isochrone fit and age determination. The lines drawn over the Pal 12 CMD are isochrones (transformed into the observational plane) for the composition $Z = 0.004$, $Y = 0.2$, and ages of 5, 7, 9, 11, 13, and 15 × 10^9 y. The luminosity and color scales for the cluster have been shifted assuming $M_V(\mathrm{HB}) = 0.9$ and $E_{B-V} = 0.02$ in order to match the models.

believe that it is most likely due to residual color errors in the photometry there. However, we are unable to correct for it specifically without having more faint calibration stars. Fortunately, our cluster age estimate depends on the fit to the turnoff region, which (internally) is much more well established.

During the fitting procedure, we allowed the heavy-element abundance Z to be a free parameter because of previous uncertainties in the first abundance indicators; similarly, we allowed minor (<0.5 mag) vertical shifts in M_V(HB) around a starting value of 0.6 in order to complete the fit. We also arbitrarily restricted the helium abundance Y to the range 0.2–0.3, which appears appropriate from other studies (Deupree *et al.* 1977; Demarque and McClure 1977), although variations in Y exerted only secondary influences on the age. From the isochrones alone values of $Z < 0.001$ could be quickly ruled out because their main sequences were far too blue and the subgiant branch too steep for any reasonable match. Forcing a fit to isochrones with [Fe/H] ≈ -1.2 ($Z = 0.001$), as might be expected from the metallicity indicators discussed in § V above, required adopting values of the other parameters which we regard as inadmissable [i.e., $Y \lesssim 0.1$, M_V(HB) ~ 2, age $\gtrsim 20 \times 10^9$ years]. We believe it is highly significant that the best isochrone match is obtained for a Z-value equivalent to the inferred *oxygen* abundance in Pal 12, [O/H] $= -0.7$ (see § V).

Our age estimate of 11×10^9 years is similar to that for 47 Tuc made by several authors (Hartwick and Hesser 1974; Demarque and McClure 1977; Carney 1980) and agrees with the physical resemblance of the two clusters. But we wish to stress that the isochrone fit must be regarded as *strictly preliminary* until a more fundamental photometric calibration of the faint main-sequence data is made. As is well known (e.g., Sandage 1970), even small systematic color shifts of $\Delta(B-V) \lesssim 0.05$, which we cannot rule out at present, would significantly alter our age estimate.

A further uncertainty relates to the evidence for the "enhanced" (nonsolar) $Z_{\rm CNO}$ abundance. A more valid estimate of the cluster age would of course require use of evolutionary tracks generated with appropriately high nonstandard values of Z(C, N, or O)/Z(total). Some initial models of this type discussed by Renzini (1977), Rood (1978), and Demarque (1979) show that the effect of enhancing C, N, or O at the same [Fe/H] appears to be mainly to redden the main sequence but to leave the giant branch almost unchanged (since the energy generation on the main sequence is adjusted, but the envelope opacities for the red giants are little affected). Some direct observational support for this prediction of constant GB temperature at constant [Fe/H], regardless of CNO, comes from the work of Pilachowski (1978). She concludes that the intermediate-metallicity clusters M3, M5, M10, and M13 all have virtually identical [Fe/H] but that M3 and M5 have enhanced CO bands compared with the other two. Yet all four clusters have identical GB colors, $(B-V)_{0,g} = 0.81 \pm 0.02$. A remaining puzzle now posed by the combination of recent theory and observation is to understand just why the giant branches of the 47 Tuc-type clusters are so much redder (by $\sim$0.1 mag) than in the M3-type clusters, given that their difference in [Fe/H] is now much smaller than was previously believed. Despite the model predictions, it may be that $(B-V)_{0,g}$ depends on $Z_{\rm CNO}$ as well as $Z_{\rm Fe}$. In any case, a set of evolutionary tracks computed with enhanced CNO at different initial Z-values would be an exceptionally valuable new resource for this entire topic (cf. more extensive comments by Carney 1980).

Unfortunately, because Pal 12 has turned out to be much nearer than implied by the earlier distance estimates, our original question whether distant halo objects ($R_{\rm GC} \gtrsim 30$ kpc) might have strong age differences cannot yet be answered directly. Age calibrations have still not yet been achieved for any clusters outside the rather restricted range of 6 kpc $\lesssim R_{\rm GC} \lesssim 15$ kpc, so that any discussions of globular-cluster age distributions that can currently be made will hardly apply to the halo as a whole. Main-sequence analyses of the intriguing outermost systems will have to await further painstaking work (and accurate photometry to $V \lesssim 24$ in some cases).

We are greatly indebted to Pierre Demarque for transmitting much of the isochrone material to us, and to Judy Cohen for early information on the red-giant abundances. Thanks go to H. Bond, P. Flower, G. Harris, and J. Hesser for comments and support at various stages of this project, to M. P. Fitzgerald for making available the University of Waterloo facilities, and to D. Pateman and P. Petrie for irreplaceable technical assistance. For financial support we are happy to acknowledge the aid of CTIO, Yale University Observatory, the University of Washington, and the National Research Council of Canada through an operating grant to W. E. H.

REFERENCES

Angeletti, L., and Giannone, P. 1979, *Astr. Ap.*, **74**, 57.
Arp, H. C. 1965, in *Galactic Structure*, ed. A. Blaauw and M. Schmidt (Chicago: University of Chicago Press), p. 401.
Arp, H. C., and Hartwick, F. D. A. 1971, *Ap. J.*, **167**, 499.
Baade, W., and Swope, H. 1961, *A.J.*, **66**, 300.
Böhm-Vitense, E., and Szkody, P. 1973, *Ap. J.*, **184**, 211.
Burbidge, E. M., and Sandage, A. R. 1958, *Ap. J.*, **127**, 527.
Canterna, R., and Schommer, R. A. 1978, *Ap. J.* (*Letters*), **219**, L119.
Carney, B. W. 1980, *Ap. J. Suppl.*, **42**, in press.
Carney, B. W., and Peterson, R. C. 1979, *Bull. A.A.S.*, **11**, 418.
Castellani, V. 1975, *M.N.R.A.S.*, **172**, 59P.
Christian, C. A., and Janes, K. A. 1979, preprint.
Ciardullo, R. B., and Demarque, P. 1977, *Trans. Yale Univ. Obs.*, **33**.
Cohen, J. G. 1979, in *I.A.U. Symposium No. 85, Star Clusters*, ed. J. Hesser (Dordrecht: Reidel), p. 385.
Cohen, J. G., Frogel, J. A., Persson, S. E., and Zinn, R. 1980, preprint.
Cousins, A. W. J. 1973, *Mem. R.A.S.*, **77**, 223.
Cowley, A. P., Hartwick, F. D. A., and Sargent, W. L. W. 1978, *Ap. J.*, **220**, 453.

Crawford, D. L., Golson, J. C., and Landolt, A. U. 1971, *Pub. A.S.P.*, **83**, 652.
Da Costa, G. S., and Freeman, K. C. 1976, *Ap. J.*, **206**, 128.
Demarque, P. 1978, private communications.
Demarque, P. 1979, in *I.A.U. Symposium No. 85, Star Clusters*, ed. J. Hesser (Dordrecht: Reidel), p. 281.
Demarque, P., and Hirshfeld, A. 1975, *Ap. J.*, **202**, 346.
Demarque, P., and McClure, R. D. 1977, in *The Evolution of Galaxies and Stellar Populations*, ed. B. M. Tinsley and R. B. Larson (New Haven: Yale University Observatory), p. 199.
Deupree, R. G., Eoll, J. G., Hodson, S. W., and Whitaker, R. W. 1978, *Pub. A.S.P.*, **90**, 53.
Dickens, R. J., and Rolland, A. 1972, *M.N.R.A.S.*, **160**, 37.
Eggen, O. J., Lynden-Bell, D., and Sandage, A. 1962, *Ap. J.*, **136**, 748.
Fitzgerald, M. P. 1969, *Astr. Ap.*, **4**, 234.
Gunn, J. E., and Griffin, R. F. 1979, *A.J.*, **84**, 752.
Harris, W. E. 1976, *A.J.*, **81**, 1095.
Harris, W. E., and Canterna, R. 1978, paper delivered at NATO Advanced Study Institute on Globular Clusters, Cambridge, England.
———. 1979, *Ap. J. (Letters)*, **231**, L19.
Harris, W. E., and Racine, R. 1979, *Ann. Rev. Astr. Ap.*, **17**, 241.
Hartwick, F. D. A. 1968, *Ap. J.*, **154**, 475.
Hartwick, F. D. A., and Hesser, J. E. 1972, *Ap. J.*, **175**, 77.
———. 1974, *Ap. J. (Letters)*, **194**, L129.
Hartwick, F. D. A., and McClure, R. D. 1972, *Ap. J. (Letters)*, **176**, L57.
Hartwick, F. D. A., and Sargent, W. L. W. 1978, *Ap. J.*, **220**, 453.
Hartwick, F. D. A., and Vanden Berg, D. A. 1973, *Ap. J.*, **185**, 887.
Hesser, J. E., and Hartwick, F. D. A. 1977, *Ap. J. Suppl*,, **33**, 361.
Iben, I. 1971, *Pub. A.S.P.*, **83**, 697.
Illingworth, G. 1976, *Ap. J.*, **204**, 73.
King, I. R. 1962, *A.J.*, **67**, 471.
———. 1966, *A.J.*, **71**, 64.
Kinman, T. D., and Rosino, L. 1962, *Pub. A.S.P.*, **74**, 499.
Kunkel, W. E. 1979, *Ap. J.*, **228**, 718.
Kunkel, W. E., and Demers, S. 1976*a*, *Ap. J.*, **208**, 932.
———. 1976*b*, in *The Galaxy and the Local Group*, *Royal Obs. Bull. No.* 182, ed. R. J. Dickens and J. E. Perry, p. 241.
Larson, R. D. 1976, *M.N.R.A.S.*, **176**, 31.
Lynden-Bell, D. 1976, *M.N.R.A.S.*, **174**, 695.
McClure, R. D., Forrester, W. T., and Gibson, J. 1974, *Ap. J.*, **189**, 409.
McCrea, W. H. 1964, *M.N.R.A.S.*, **128**, 147.
Norris, J., and Zinn, R. 1975, *Ap. J.*, **202**, 335.
Peterson, C. J. 1976, *A.J.*, **81**, 617.
Peterson, C. J., and King, I. R. 1975, *A.J.*, **80**, 427.
Pilachowski, C. A. 1978, *Ap. J.*, **224**, 412.
———. 1979, in *I.A.U. Symposium No. 85, Star Clusters*, ed. J. Hesser (Dordrecht: Reidel), p. 467.
Racine, R. 1969, *A.J.*, **74**, 1073.
———. 1971, *Ap. J.*, **168**, 393.
———. 1975, *A.J.*, **80**, 1031.
Renzini, A. 1977, in *Advanced Stages in Stellar Evolution*, proc. of Seventh Advanced Course of the Swiss Society of Astronomy and Astrophysics, ed. P. Bouvier and A. Maeder (Sauverny: Geneva Observatory).
Rood, R. 1978, paper delivered at NATO Advanced Study Institute on Globular Clusters, Cambridge, England.
Rood, R., and Iben, I. 1968, *Ap. J.*, **154**, 215.
Saio, H. 1977, *Ap. Space Sci*, **50**, 93.
Sandage, A. 1957, *Ap. J.*, **125**, 422.
Sandage, A. 1970, *Ap. J.*, **162**, 841.
Sandage, A., and Smith, L. L. 1966, *Ap. J.*, **144**, 886.
Sandage, A., and Wallerstein, G. 1960, *Ap. J.*, **131**, 598.
Sandage, A., and Wildey, R. 1967, *Ap. J.*, **150**, 469.
Searle, L., and Zinn, R. 1978, *Ap. J.*, **225**, 357.
Sneden, C., Lambert, D. L., and Whitaker, R. W. 1979, *Ap. J.*, **234**, 964.
Spitzer, L., and Shull, J. 1975, *Ap. J.*, **201**, 773.
Stetson, P. B. 1979, *A.J.*, **84**, 1149.
Stetson, P. B., and Harris, W. E. 1977, *A.J.*, **82**, 954.
Strom, S. E., Strom, K. M., and Bregman, J. N. 1971, *Pub. A.S.P.*, **83**, 768.
Sweigart, A. V., and Gross, P. G. 1976, *Ap. J. Suppl.*, **32**, 367.
Wheeler, J. C. 1979, *Ap. J.*, **234**, 569.
Woolf, N. J. 1964, *Ap. J.*, **139**, 1081.
Zinn, R. 1978, paper delivered at NATO Advanced Study Institute on Globular Clusters, Cambridge, England.

R. Canterna: Department of Physics and Astronomy, University of Wyoming, Laramie, WY 82071

W. E. Harris: Department of Physics, McMaster University, Hamilton, Ontario L8S 4M1, Canada